Capillary penetration in cells with periodical corrugations

F.A. Sánchez

FIME Universidad Autónoma de Nuevo León,
Ciudad Universitaria, San Nicolás de los Garza, N.L., 66451, México.

G.J. Gutiérrez and A. Medina

SEPI-ESIME Azcapotzalco, Instituto Politécnico Nacional,
Av. de las Granjas #682, Col. Sta. Catarina, México D.F., 02250, México.

In this work we present a theoretical study of the spontaneous capillary flow of a viscous liquid, developed in the gap between a couple of parallel corrugated plates (corrugated Hele-Shaw cell). The periodical corrugation of the interior walls of the plates is assumed as a sine-like pattern, transverse to the flow direction. Such a configuration may generate periodical gaps with a structure where zones of maximum and minimum closing occur. This is a simple idealization of typical micro and nano fabricated gaps used to mould polymers by capillarity. This model can also be useful to understand the capillary flow in naturally fractured reservoirs. By using lubrication theory we found that a very peculiar temporal flow is developed which could be of interest in improving our knowledge of this type of moulding.

Keywords: Micro and nano-scale flow phenomena; capillary effects; flow in channels.

En este trabajo presentamos un estudio teórico del flujo capilar espontáneo, de un líquido viscoso, desarrollado en el espacio entre un par de placas paralelas (celda de Hele-Shaw corrugada). La corrugación periodica de las paredes interiores se supone como patrones tipo seno, transversa a la dirección de flujo. Tal configuración puede generar espacios periódicos con estructuras de máximo y mínimo acercamiento entre ellas. Esta es una idealización simple de los típicos espacios micro y nanofabricados usados para moldear polímeros por capilaridad. Este modelo también puede ser útil para entender el flujo capilar en yacimientos naturalmente fracturados. Usando la teoria de la lubricación encontramos que se desarrolla un peculiar flujo capilar temporal el cual puede ser de interés para mejorar nuestro conocimiento sobre este tipo de moldeo.

Descriptores: Fenómenos de flujo a micro y nano escala; efectos capilares; flujo en canales.

PACS: 47.61.-k; 47.55.nb; 47.60.+i

1. Introduction

This work considers the dynamics of the capillary penetration of a viscous liquid into a corrugated Hele-Shaw cell. By using this configuration the authors have previously analyzed the equilibrium height (equilibrium free surface) attained by a liquid when the corrugation in the cell is assumed to have a sine-like structure, transverse to the main flow direction, which is along the vertical direction [1]. The equilibrium height was reached when the capillary and hydrostatic pressures were balanced.

In our previous work we have argued that this basic configuration allows us to generate complex free surfaces. In this work we study the dynamic evolution of such free surfaces and how the equilibrium profiles are reached as a function of time. This problem completes the study of how a viscous liquid can spontaneously penetrate, due to the action of the capillary pressure, vertical, structured two-dimensional channels. Physically, the characteristic spatial scale where the capillary pressure acts is of the order of the capillary length, $l_c = (\sigma/\rho g)^{1/2}$, where σ is the surface tension, ρ is the liquid density and g is the gravity acceleration. In normal terrestrial conditions the capillary length is of the order of a few millimeters. Thus, our study can be useful in understanding flows in micro and nano fabricated gaps used to mould polymers by capillarity [2] and in modeling the capillary flows

in naturally fractured reservoirs of oil and gas and flows in fractured rock aquifers, which are of enormous economical importance [3].

In modeling the *film flow* developed in the corrugated Hele-Shaw cell we have used the lubrication theory [4]. By using this approximation, we can follow the two-dimensional flow whose main directions are along the vertical direction and along the direction where the corrugation occurs. Due to the high non-linearity of the resulting equations we have solved they numerically. Through the resultant free surfaces and the times involved in reaching equilibrium, we show that the geometry imposes strong periodical deformations on the interface and that the spatially averaged profile, $\widehat{H}_{av}$, evolves as a function of time, τ, approximately obeying, for short times, the Washburn law where $\widehat{H}_{av} \propto \tau^{1/2}$. Incidentally, this law is valid in spontaneous capillary flows without corrugation and in the absence of gravity.

The division of this work is as follows: in the next section we derive the governing equations to describe the film flow in the cell. After that, in Sec. 3 we discuss the numerical solutions for the spatially averaged profiles and for the time elapsed to attain the equilibrium height. Finally, in Sec. 4 we present the main conclusions of this work.
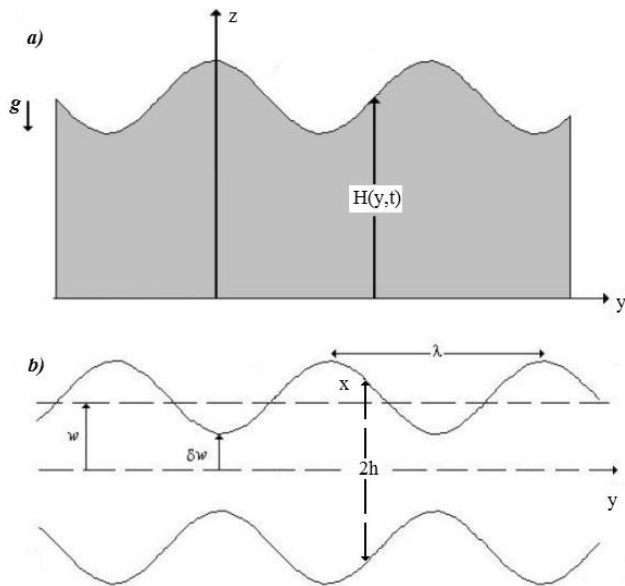
FIGURE 1. a) Schematic view of the zone invaded by a viscous liquid (grey zone). $H(y,t)$ denotes the air-liquid interface. b) Gap between the corrugated walls. The main geometrical parameters of the corrugation are shown.
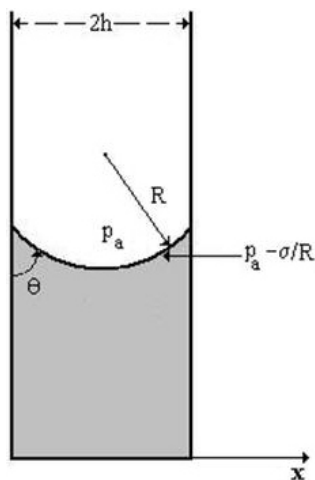

FIGURE 2. Local shape of the liquid between plates where contact angle θ is shown. Here the curvature radius R and the value of the pressure on the free surface are defined.

2. Governing equations for spontaneous capillary penetration

Physically, spontaneous capillary penetration of a liquid into a vertical nano or micro channel, of characteristic size a, is due to the capillary pressure $p_c \sim \sigma/a$ which pulls the liquid up into the capillary. In vertical channels the flow should be finally stopped at the equilibrium height H where the hydrostatic pressure compensates the capillary pressure [5, 6]. In a Hele-Shaw cell, made of two parallel flat plates close together, the equilibrium profile is a horizontal flat surface $z = H = constant$, where z is the upward vertical coordinate.

In this work, we assume that the interior walls of the corrugated Hele-Shaw cell have a sine-like corrugation. Our purpose in this part is to understand how such a corrugation changes the shape of the liquid free surface. In order to analyze this problem we assume that the flow in the corrugated cell is a thin film or lubricated flow, because the maximum amplitude of the corrugation is so small that it allows the development of such a flow. In Fig. 1 we consider the vertical Hele-Shaw cell with corrugated walls.

Qualitative experiments [1] allow us to observe that the flow has a free surface as shown in Fig. 1a. For simplicity, we suppose that each plate has a sine-like corrugation given by

$$h(y) = \pm w \left[1 - (1 - \delta) \cos \frac{2\pi y}{\lambda} \right], \tag{1}$$

where $h = w\delta$ is the minimum amplitude of the corrugation, $h = 2w - w\delta$ is the maximum amplitude and λ is the wavelength of the corrugation. The coordinate system is (x, y, z) as shown in Fig. 1a and 1b.

Notice that a system of flat parallel plates a distance $2w$ apart are obtained for $\delta = 1$, and the amplitude of the corrugation is maximum for $\delta = 0$. To build the capillary pressure that yields the motion of the liquid we assume that locally, across the transversal direction, x, the free surface is made of sections of spheres with curvature $R = h/\cos\theta$ where θ is the contact angle. (See Fig. 2). Then the capillary pressure in the free surface is $p_c = p_a - \sigma/R = p_a - 2\sigma\cos\theta/h(y)$ where p_a is the atmospheric pressure and $h(y)$ indicates explicitly that the separation between plates is a function of y.

When the liquid advances it does not cross the free surface $f(z, y, t) = z - H(y, t) = 0$; this is the deep-averaged kinematic condition which yields an equation for the deep-averaged free surface, f (see Fig. 1a) in the form

$$-\frac{\frac{\partial f}{\partial t}}{|\nabla f|} 2h = \mathbf{q} \cdot \mathbf{n} = \mathbf{q} \cdot \frac{\nabla f}{|\nabla f|}, \tag{2}$$

where $\mathbf{n}$ is the unit vector normal to the surface pointing inside, $\mathbf{q}$ is the volume flowrate vector per unit length, and $\mathbf{q} = (q_y, q_z)$. The simplification of Eq. (2) gives

$$-\frac{\partial f}{\partial t} 2h = \mathbf{q} \cdot \nabla f, \tag{3}$$

where q_y and q_z are, respectively,

$$q_y = -\frac{(2h)^3}{12\mu} \frac{\partial p}{\partial y}, \tag{4}$$

$$q_z = -\frac{(2h)^3}{12\mu} \frac{\partial p}{\partial z}; \tag{5}$$

here μ is the dynamic viscosity. In terms of (q_y, q_z) the mass conservation can be written as

$$\frac{\partial q_y}{\partial y} + \frac{\partial q_z}{\partial z} = 0. \tag{6}$$

The use of relations (4) and (5) in (6) yields the Reynolds equation for the pressure

$$\frac{\partial}{\partial y}\left(h^3\frac{\partial p}{\partial y}\right) + \frac{\partial}{\partial z}\left(h^3\frac{\partial p}{\partial z}\right) = 0, \tag{7}$$

which will be solved under the boundary conditions

$$p = 0 : \text{ at } z = 0, \tag{8}$$

$$p = -\frac{2\sigma\cos\theta}{h(y)} + \rho g H : \text{ at } z = H(y,t), \tag{9}$$

$$p(y,z) = p(y+\lambda,z). \tag{10}$$

Equation (8) expresses the condition that the pressure p is the pressure of the liquid referred to the pressure of the surrounding gas (p_a), Eq. (9) refers to the condition that the pressure at the free surface is the sum of the capillary pressure plus the hydrostatic pressure and, finally, Eq. (10) is the condition of periodicity for the pressure.

Given a free surface, Eq. (7) yields the pressure field in the liquid. The free surface then is advanced by the kinematic condition [6] which in terms of H has the form

$$\frac{\partial H}{\partial t} = \frac{h^2}{3\mu}\frac{\partial p}{\partial y}\frac{\partial H}{\partial y} - \frac{h^2}{3\mu}\frac{\partial p}{\partial z}. \tag{11}$$

Coupled Eqs. (7) and (11) need to be solved numerically because there are no analytical solutions for them. In order to get such solutions we transform Eqs. (7) and (11) and boundary conditions (8)-(10) into their non-dimensional form. The adequate dimensionless variables are

$$\widehat{H} = \frac{H}{z_e}, \tau = \frac{t}{t_c}, \xi = \frac{x}{w}, \eta = \frac{y}{\lambda},$$

$$\zeta = \frac{z}{z_e}, \widehat{h} = \frac{h}{w}, \widehat{p} = \frac{p}{p_c}, z_e = \frac{\sigma\cos\theta}{\rho g w}. \tag{12}$$

The quantity z_e is the equilibrium height attained by the free surface if the corrugation does not exist. In terms of these quantities, Eq. (7) for the pressure transforms into the dimensionless equation

$$\frac{\partial}{\partial\eta}\left(\widehat{h}^3\frac{\partial\widehat{p}}{\partial\eta}\right) + \frac{\lambda}{z_e}\frac{\partial}{\partial\zeta}\left(\widehat{h}^3\frac{\partial\widehat{p}}{\partial\zeta}\right) = 0, \tag{13}$$

while Eq. (11) takes the non-dimensional form

$$\frac{\partial\widehat{H}}{\partial\tau} = \frac{\widehat{h}^2}{3}\frac{\partial\widehat{p}}{\partial\eta}\frac{\partial\widehat{H}}{\partial\eta} - \frac{\lambda}{z_e}\frac{\widehat{h}^2}{3}\frac{\partial\widehat{p}}{\partial\zeta}, \tag{14}$$

and the derivation of Eqs. (13) and (14) allows us to establish that $p_c = \sigma\cos\theta/w$ and $t_c = \mu\lambda^2/(w\sigma\cos\theta)$. In addition, Eqs. (13) and (14) will be solved under the dimensionless boundary conditions

$$\widehat{p} = 0 : \text{at } \zeta = 0, \tag{15}$$

$$\widehat{p} = \widehat{H} - \frac{1}{\widehat{h}} : \text{at } \zeta = \widehat{H}, \tag{16}$$

$$\widehat{p}(\eta,\zeta) = \widehat{p}(\eta+1,\zeta). \tag{17}$$

3. Results

The resulting system of partial differential equations (13)-(14) subjected to the boundary conditions (15)-(17) was solved by using the implicit finite-differences discretization. A careful analysis of the solutions as a function of the spatial and temporal meshes allows us to know that a 50×50 mesh is adequate to get an accurate solution. The numerical time step was variable; in the first stages of the phenomenon the time step was around 10^{-9} and it was increased as the phenomenon advanced. Typical calculations were made for a total of 20 000 time steps.
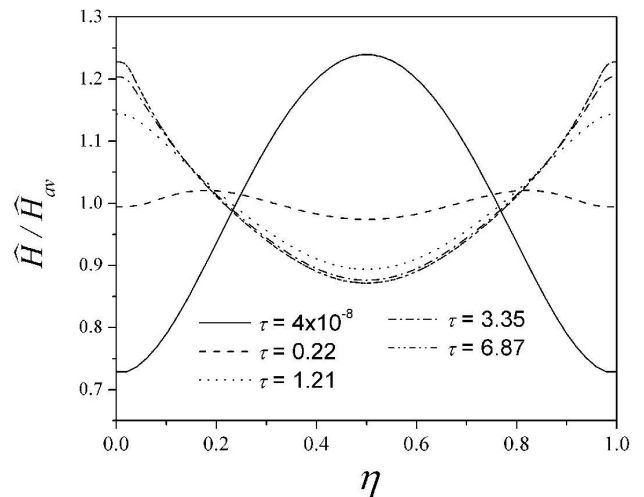

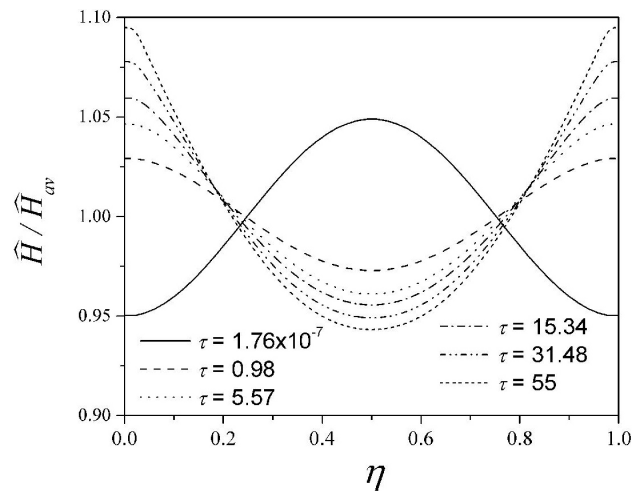FIGURE 3. Free surfaces for several dimensionless times τ. Here $\lambda/z_e = 0.01$ and $\delta = 0.5$.

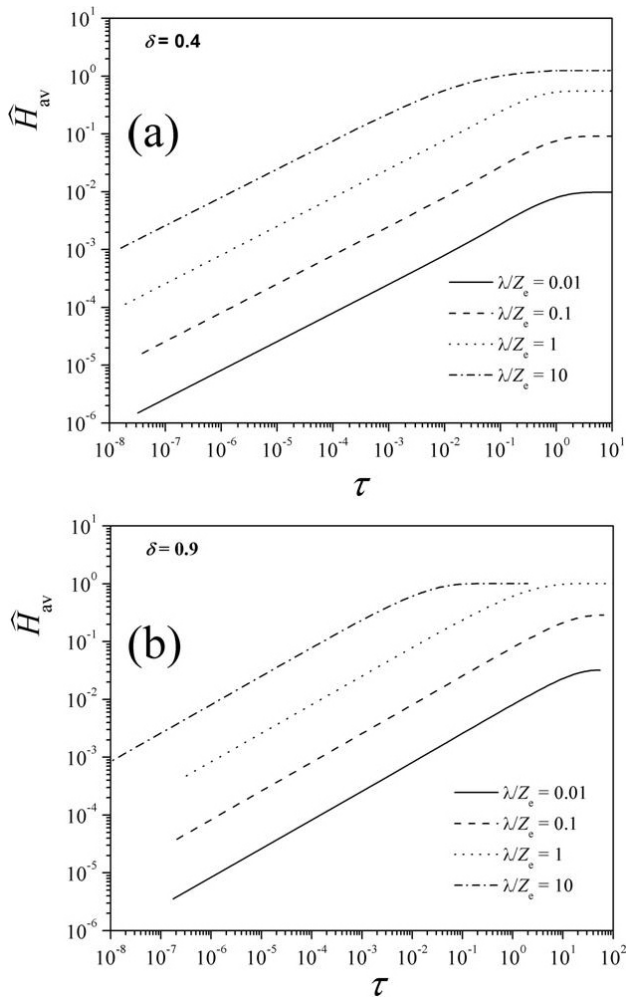FIGURE 4. Free surfaces for several dimensionless times τ. Here $\lambda/z_e = 0.01$ and $\delta = 0.9$.

FIGURE 5. Log-Log plot of the dimensionless averaged height $\widehat{H}_{av}$ as a function of the dimensionless time τ. In (a) the value $\delta = 0.4$ implies that the corrugation is stronger than in (b) where $\delta = 0.9$.

3.1. Free surface evolution

In Figs. 3 and 4 we show the time evolution of the dimensionless normalized free surface profiles $\widehat{H}/\widehat{H}_{av}$ as a function of η for several dimensionless times, τ. $\widehat{H}_{av}$ is the spatially averaged height, reached at time τ, and is defined as

$$\widehat{H}_{av} = \int\limits_0^1 \widehat{H}(\eta)d\eta.$$

Figure 3 shows the transient evolution of the free surface for $\lambda/z_e = 0.01$ and $\delta = 0.5$. At short times, the free surface penetrates faster in the zone where plates are more separated ($\eta = 0.5$) and, as time elapses, the free surface in this zone reduces their speed and finally it is delayed with respect to the free surface located in zones where plates are closer ($\eta = 0, 1$). This peculiar behavior has been also observed during the capillary penetration of a viscous liquid between a couple of vertical plates making a small angle [7] (Taylor's problem [8]) where initially the free surface of the liq-

uid reaches a maximum height close to the union of the plates and slowly this maximum advances to the zone of contact of the plates. Formally, this latter case can be seen as locally valid for zones where $\eta = 0, 1$. Consequently, the change in the curvature of the free surface as a time function can be explained as due to the strong shear stresses that initially are stronger in the zones where plates are closer. There the shear stresses overcome the capillary driven force that always pulls up the free surface.

Figure 4 shows the temporal behavior of the free surface when corrugation is very smooth ($\delta = 0.9$). As in Fig. 3, it has been assumed in this plot that the wavelength of the corrugation is short ($\lambda/z_e = 0.01$). Another interesting result is observed from the estimation of the averaged height, $\widehat{H}_{av}$, as a time function. This quantity is a measure of how, on average, the free surface of the liquid advances into the corrugated cell. In Fig. 5 we observe that $\widehat{H}_{av}$ is nearly independent of factor δ, which is related to the intensity of the
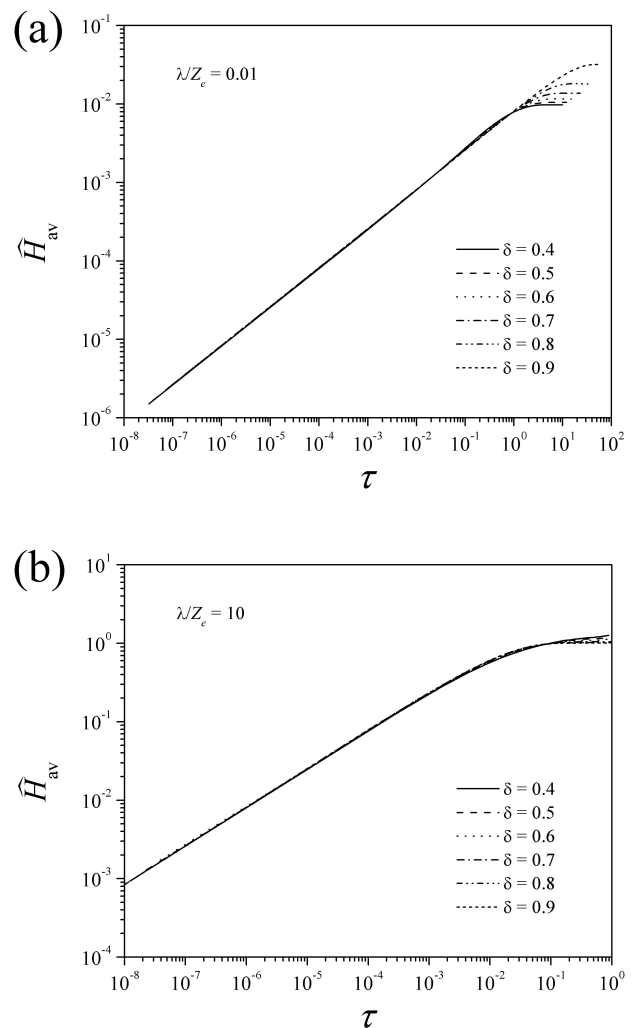

FIGURE 6. Log-log plots of $\widehat{H}_{av}$ as a function of the dimensionless time τ. (a) corresponds to corrugations of short wavelength and several amplitudes δ. (b) corresponds to corrugations of large wavelength for the same values of δ as in (a).

corrugation. Moreover, it is observed that the averaged height depends strongly on the wavelength λ, *i.e.*, large λ implies high $\widehat{H}_{av}$. Also, in Fig. 5 we indeed note that the dimensionless time elapsed to attain the respective equilibrium height (height where the curve transforms into a horizontal line) is shorter as λ is larger.

3.2. Times to attain the equilibrium height

At short times the log-log plot of $\widehat{H}_{av}$ vs τ, in Fig. 5, yields for all cases the power law $\widehat{H}_{av} \propto \tau^{0.4837}$, *i.e.*, this behavior is very similar to that found in the capillary penetration of viscous liquids into Hele-Shaw cells without corrugation where at short times $\widehat{H}_{av} \propto \tau^{1/2}$. This result is known as the Washburn law and it is also valid for capillary penetration in pipes and Hele-Shaw cells in the absence of gravity [9].

By the way, Fig. 6 shows very important results related also to the averaged height but now when the wavelength is maintained constant. In Fig. 6a we plot $\widehat{H}_{av}$ vs τ for $\lambda/z_e = 0.01$ and several values of δ. These cases correspond to corrugated cells where the separation between maxima is very short. Conversely, in Fig. 6b is shown the plot for $\lambda/z_e = 10$, which means that the separation between maxima is large. The main conclusion derived from plots in Fig. 6a is that the free surface, for short wavelengths, and strong corrugation ($\delta = 0.4$), attains an averaged equilibrium height lower than that corresponding to the case of smooth corrugation, when $\delta = 0.9$. Consequently, the time needed to attain this height is lower (around an order of magnitude) for the case of strong corrugation than that corresponding to smooth corrugation and equal wavelength. It means that periodical strong corrugation, of short wavelength, encourages the liquid to saturate the cell faster than the saturation of a cell corrugated with a smooth corrugation. Moreover, the volumes of saturation are different and are higher in a smooth cell. Surprisingly, when the wavelength is large (Fig. 6b) those effects are not observed.

4. Conclusions

In this work we have presented a simple model for analyzing the dynamics of the spontaneous capillary penetration of a liquid into periodically corrugated Hele-Shaw cells. These types of cells are similar to those occurring, for instance, in molding of polymer in continuous networks of nano and micro channels [2]. The model of corrugated cells also can be of importance to model flow in fractures during the enhanced oil recovery by the method of imbibition, where a liquid or gas is displaced capillary by an other liquid [3]. In this context, an important result is that despite the corrugation and under the gravity field, the spatially averaged height, $\widehat{H}_{av}$, very approximately obeys the Washburn law, *i.e.*, $\widehat{H}_{av} \propto \tau^{1/2}$.

By the way, the set of partial differential equations were derived using the lubrication approximation valid for a film flow developed in the corrugated cells. The partial differential equations were solved using the implicit finite-difference method. As a result a very detailed spatial and temporal description of the free surface was achieved.

We have found that the curvature of the free surface evolves in a complex way as the liquid penetrates into the cell. The time evolution of the averaged free surface shows how the wavelength, λ, and the corrugation factor, δ, determine different ways of capillary penetration or evolution of the averaged height $\widehat{H}_{av}$. These mechanisms could be of interest in the modeling of spontaneous capillary penetration in complex channels that can be approximated by our model of periodically corrugated Hele-Shaw cells.

Acknowledgements

1. M. Francisco, A. Medina, F.A. Sánchez, and F.J. Higuera, *Rev. Mex. Fís.* **52** (2008) 247.

2. E. Kim, Y. Xia, and G. Whitesides, *Nature* **376** (1995) 581.

3. P. Dietrich *et al.*, *Flow and transport in fractured porous media*, (Springer, Berlin, 2005).

4. A.Z. Szeri, *Fluid film lubrication: theory and design* (Cambridge University Press, Cambridge, 2005).

5. P.-G. de Gennes, F. Brochard-Wyart, and D. Quere, *Capillarity and Wetting Phenomena: Drops, Bubbles, Pearls, Waves* (Springer, Berlin, 2004).

6. S. Middleman, *Modeling Axisymmetric Flows*, (Academic Press, San Diego, 1995).

7. F.J. Higuera, A. Medina, and A. Liñán, *Phys. Fluids* **20** (2008) 102102.

8. B. Taylor, *Philos. Trans. R. Soc. London* **27** (1712) 538.

9. M. Sánchez, F. Sánchez, A. Medina, C. Pérez-Rosales, and C. Treviño, *Phys. Lett. A* **324** (2004) 14.